

N 7 4 1 0 0 2 1

**NASA TECHNICAL
MEMORANDUM**

NASA TM X- 71460

NASA TM X- 71460

**CASE FILE
COPY**

**SOME DESIGN CONSIDERATIONS FOR SUPERSONIC
CRUISE MIXED COMPRESSION INLETS**

by David N. Bowditch
Lewis Research Center
Cleveland, Ohio 44135

TECHNICAL PAPER proposed for presentation at
Propulsion Joint Specialist Conference sponsored by
the American Institute of Aeronautics and Astronautics
and the Society of Automotive Engineers
Las Vegas, Nevada, November 5-7, 1973

SOME DESIGN CONSIDERATIONS FOR SUPERSONIC CRUISE MIXED COMPRESSION INLETS

by David N. Bowditch
Chief, Propulsion Aerodynamics Branch
Lewis Research Center
National Aeronautics and Space Administration
Cleveland, Ohio

SUMMARY

A mixed compression inlet designed for supersonic cruise has very demanding requirements for high total pressure recovery and low bleed and cowl drag. However, since the optimum inlet for supersonic cruise performance may have other undesirable characteristics, it is necessary to establish trade-offs between inlet performance and other inlet characteristics. The paper will review some of these trade-offs between the amount of internal compression, aerodynamic performance and angle-of-attack tolerance. Also some techniques in use at the Lewis Research Center for analysis of boundary layer control and subsonic diffuser flow will be discussed.

INTRODUCTION

Within the last 10 years, a considerable amount of supersonic cruise inlet work has been under way within industry and government (ref. 1-28). Each inlet research group seems to prefer a given type of inlet which is either two-dimensional or axisymmetric with collapsing or translating centerbodies. Each type has its own advantages both from an aerodynamic or mechanical standpoint. These make a given inlet more adaptable to one aircraft configuration than another. Therefore it is necessary to be able to evaluate the effect of each inlet type on aircraft range so that its characteristics can be traded against other characteristics of the configuration. The effect of the inlet aerodynamic characteristics on aircraft range will be considered at Mach 2.5 and a correlation of bleed requirements from data available in the open literature will be presented. A summary of the airflow matching and angle of attack characteristics will also be discussed.

Better analytical tools are becoming available for design of supersonic inlets. These include improved computer programs for axisymmetric characteristics and improved boundary layer analysis. Also computer analysis of the subsonic diffuser is available. The Lewis Research Center through in-house develop-

ment, contract, and grant is acquiring inlet design computer programs which should eventually permit the calculation of viscous and inviscid inlet flows from the free stream to the compressor face. The programs will be generally available and will handle angle of attack for some cases. The results of some recent experience on use of programs for predicting the subsonic diffuser flow and the boundary layer development in the supersonic diffuser will be reviewed.

EFFECT OF INTERNAL COMPRESSION ON INLET CHARACTERISTICS

A few of the inlets tested in the last few years are shown in figure 1. While the design Mach numbers vary from only 2.5 to 2.7, it can be seen that the internal compression varies from a low of 35 percent for the two-dimensional inlet to 80 percent for an axisymmetric inlet. The parameter of internal compression used in this paper, is defined as that portion of the supersonic area contraction that occurs inside the cowl lip. The high internal compression of 80 percent is needed to keep the centerbody small so that when it is translated forward, a maximum annular area can be obtained at the cowl lip for matching an engine at transonic speeds where its airflow requirements are largest. The axisymmetric inlet with 65 percent internal compression has about the minimum amount to avoid significant losses in recovery of the shock from the cowl lip or a cowl angle larger than zero degrees which would incur drag. This inlet must have a collapsing centerbody to provide normal engine flows at transonic speeds. The inlet with 48 percent internal compression has about the least that is compatible with acceptable total pressure recovery and cowl drag losses in exchange for other characteristics which will be discussed. The two-dimensional inlet represents a similar compromise.

RANGE

To investigate the aerodynamic tradeoffs associated with different amounts of internal compression, axisymmetric inlets were studied at a Mach number of 2.5. Tradeoffs for other Mach numbers and inlet types will have similar trends. For an axisymmetric inlet, an inherent effect on the recovery and cowl drag is associated with the choice of internal compression. As this internal compression is reduced, the increased external compression caused higher flow angles at the cowl lip. This requires a tradeoff between strengthening the oblique shock from the cowl lip and increasing the cowl lip angle which results in reduced recovery and a higher cowl drag, respectively. Figure 2

presents this variation in recovery and cowl drag as a function of internal compression. To make the curve, the ratio of internal flow area to the outside nacelle area at the compressor face was chosen equal to the Boeing 2707 configuration. Also the effect of inlet total pressure recovery on inlet capture area and projected cowl area and drag is included. The curves are for the optimum cowl lip angle giving maximum range. For the optimization, increments obtained from mission studies and reported in reference 22 were used (0.01 in total pressure recovery and cowl drag are equivalent to 32 and 41 nmi range, respectively). It can be seen that variation in cowl drag and recovery with internal compression is negligible at values above about 60 percent. Also at values below about 35 percent internal compression, the recovery and drag penalties become prohibitive as the cowl lip oblique shock turning is forced above 12° .

The external and internal supersonic compression, other than the cowl lip oblique shock, can be as isentropic as the ingenuity of the mechanical and aerodynamic designers can provide. Therefore, the only recovery and cowl drag change inherent in the choice of internal compression is associated with the cowl lip oblique shock. In the subsequent comparison, the recovery variation will be the only one considered.

The remaining factor inherently associated with the internal compression choice is bleed flow. An initial idea of this effect on bleed is given in figure 3 which presents the supersonic diffuser wetted area as a function of capture area. The wetted areas in this figure were obtained by utilizing coordinate data obtained from the respective reports. The data points each represent an inlet of the designated design Mach number. Table I lists the inlets by their report number, when available, and also presents the pertinent data used in paper. In general, all the axisymmetric inlets (circles) with conventional distributed compression systems fall along a single line. Two exceptions are at Mach 3.5 and 2.5. At Mach 3.5, the inlet falling on the correlation line was designed with a relatively short supersonic diffuser. However, the inlet could not provide proper transonic flow matching for a turbojet engine. A lengthened inlet, upper flagged circle, solved the matching problem but at the expense of an increase in wetted area. For the Mach 2.5 inlets at 47.5 percent internal compression, the symbols falling below the line represent inlets with focused internal compression which provides the shortest possible internal supersonic diffuser.

For two-dimensional inlets, the ratio of the wetted area of the supersonic diffuser, A_{wSD} , to the capture area, A_C , can

be expressed as

$$\frac{A_{WSD}}{A_C} = \frac{A_{WCR}}{A_C} + \frac{A_{WSw}}{h^2} \frac{1}{AR}$$

where A_{WCR} is the wetted area of the cowl and ramps, A_{WSw} is the side wall wetted area, the aspect ratio, AR , is the ratio of the inlet width to the verticle height from the ramp tip to the cowl lip, h , and the capture area, A_C is equal to the product of the same inlet height and width. Therefore, for a two-dimensional inlet, the ratio of the total wetted area of the supersonic diffuser to the capture area decreases as the inlet aspect ratio increases. A second flagged point is therefore plotted in figure 3 for each two-dimensional inlet and corresponds to an inlet of aspect ratio one with the same aerodynamic design.

In general, both the axisymmetric and two-dimensional data correlate well with a linear increase of wetted area with increasing internal compression. The two-dimensional inlets also have almost twice the wetted area of the axisymmetric inlets. The correlation lines were used in conjunction with the next curve to estimate the variation in bleed flow with internal compression.

To equate bleed with wetted area, it is necessary to choose an equivalent operating point on each of the inlet pressure-recovery, mass-flow curves to obtain a representative bleed flow. With the diverse designs of supersonic and subsonic diffusers represented by the available inlet data, this is a difficult job at best. For the current study, the criteria was based on choosing from the reported data, the combination of bleed and recovery that provided the maximum range (range increments based on 0.01 in total pressure recovery and bleed flow equaling 32 and 29 miles, respectively. Bleed incremental range was based on an average bleed recovery of 0.20). The resulting bleed flow is shown on figure 4, as a function of the wetted area divided by the inlet throat area. For consistency, the throat area for figure 4 was obtained by multiplying the inlet capture area by the ratio of the isentropic area ratios for free stream Mach number and a throat Mach number of 1.25. This provides a consistent, simple method of converting the ratio of wetted area to capture area from figure 3 to the ratio of wetted to throat area of figure 4. A suprisingly consistent trend can be seen in the figure, particularly when considering that it includes inlets designed for Mach numbers from 2.5 to 3.5 and both two-dimensional and axisymmetric inlets. The correlation line on the figure

combined with figure 3 represents the basis for estimating inlet bleed flow variation with internal compression. In the near future it should be possible to calculate this curve which will provide a more solid basis, but the inability to analytically handle the boundary layer in the terminal shock region currently prevents that.

Based on the three prior curves, the effect of the internal compression of a Mach 2.5 axisymmetric inlet on supersonic cruise range is presented in figure 5. The range calculation procedure assumed GE4 engine flow and the ratio of compressor face to nacelle area equal to that of the Boeing 2707 pod. These assumptions were necessary to determine the cowl drag back to the engine face station. The cowl drag was adjusted for inlet recovery changes which change inlet capture area and projected cowl area. A nominal total pressure recovery of 0.928 was used and the recovery increments from figure 2 were applied to that value. The open circles represent Lewis axisymmetric inlets designed for Mach 2.5 and the solid circles represent Ames and Boeing SST inlets designed for Mach 2.65. The bleed flows of the Mach 2.65 inlets were adjusted to a Mach 2.5 value by multiplying the actual bleed flow at Mach 2.65 by the ratio of the capture to throat areas corresponding to Mach 2.5 and 2.65. The predicted range variation tends to be verified by the location of the individual inlet ranges which are based on their individual recovery, bleed and cowl drag. Because of the difficulty in estimating the cowl drag of a two-dimensional inlet, the two dimensional inlet is presented in figure 5 at the higher values of internal compression where the cowl drag is not significantly different from the lowest axisymmetric value. However, due to their larger wetted area, a range reduction of 165 miles is obtained for bleed alone.

In general, the resulting curve on figure 5 indicates a broad range of internal compression where the various aerodynamic characteristics of the inlet trade off to provide about constant range. Therefore, other inlet characteristics such as angle of attack performance, weight, complexity, etc., will be more important in the choice of inlet design. Two-dimensional inlets, however, due to their larger bleed requirement, appear to have an inherent penalty of about 100 miles range when compared to similar axisymmetric inlets.

AIRFLOW MATCHING

Another consideration affecting inlet choice is the way it matches the chosen engine cycle. In the past there has been a

rather limited variation in engine cycles which all approached the turbojet cycle matching characteristics presented in figure 6. Here the ratio of throat to capture areas required to match a turbojet engine is presented for both the design Mach number and transonic conditions. These usually represent the extremes in required throat area variation for providing the required engine airflow. In recent AST studies, emphasis has generally been applied to increasing the subsonic engine airflow to lower jet velocities and reduce take off noise. Increased flow curves are presented for comparison with the throat area variation capability of existing inlets. In general, the translating centerbody inlets are limited in transonic airflow capacity and can only provide the full transonic airflow of a turbojet for the higher design Mach numbers. The two-dimensional and axisymmetric collapsing centerbody inlets (solid symbols) have been plagued with providing too much flow in the past. Therefore, their excess flow capacity has probably been minimized for the designs presented here, and larger transonic flows are possible, particularly for the two-dimensional inlets. Therefore, to provide added transonic flow for an advanced supersonic cruise engine, some form of collapsible inlet will probably be required.

ANGLE OF ATTACK

Experimentally it has been observed that the angle of attack of an axisymmetric mixed compression inlet is limited by inlet unstart associated with choking of the flow in the supersonic diffuser. No matter how far supercritical an inlet is operated, there is a maximum angle of attack at which the inlet can be operated in a started mode with the optimum geometry for zero angle of attack. Lesser angle of attack limits are observed when the inlet is operating near peak, but it is the maximum value at supercritical conditions that is considered here. While the cause of the limit cannot be fully explained, the experimentally observed effects for an axisymmetric inlet are shown in figure 7. The shock structure on the leeward side of the inlet and the corresponding pressure distribution are shown at zero and maximum angle of attack. As angle of attack is increased, the oblique shock structure moves forward on the leeward side of the inlet which is indicative of added compression. The angle of attack limit is reached when a subsonic region, indicated by pressures greater than the sonic value, grows large enough to choke the flow and causes inlet unstart. This over compression can be alleviated by forward bleed, providing larger angle of attack.

In several cases, the angle of attack limit has coincided with the overcompressed region reaching the upstream edge of a bleed region. However, this added bleed causes extra drag during normal cruise.

The overcompression on the leeward side of the inlet has two potential sources; (1) the boundary layer migration normally associated with conical forebodies at angle of attack with resulting throat blockage, and (2) the inviscid flow field. With the currently available computer programs it is not possible to determine the degree that the viscid and inviscid flows play in limiting angle of attack. Work is needed to improve the understanding of inlet operation at angle of attack and it has the potential for improving maximum unstart angle of attack and the distortion at high angles of attack. A three-dimensional analysis of both the inviscid and viscous flows is needed. For the two-dimensional inlet, angle of attack relative to the ramps is limited because it increases the overall compression causing choking at the throat. Therefore, an angle of attack limit equal to the Prandtl Meyer angle corresponding to the throat Mach number (4.8° for 1.25 Mach number) would be expected.

The experimentally demonstrated variation of unstart angle of attack limit with internal compression is presented in figure 8. The cross hatched band represents experience from various bleed configurations with near optimum performance bleed. For axisymmetric inlets, high internal compression limits the demonstrated angle of attack tolerance to only several degrees. Less internal compression appears to provide a more desirable angle of attack unstart limit. The two-dimensional inlet angle of attack tolerance is for angle relative to the ramps. The maximum angle of attack limit at 35 percent internal compression corresponds to the expected angle of attack limit for a throat Mach number of 1.25.

SUPERSONIC DIFFUSER BLEED ANALYSIS

A program has been proceeding at Lewis Research Center to develop analytical methods for estimating the development of the boundary layer in the inlet and the necessary bleed flow for insuring its good behaviour (ref. 29). The method in current use involves patching an inviscid characteristics analysis with a boundary analysis. The procedures are similar to those of references 26 to 28 but utilize generally available computer programs. The numerical analysis of MacDonald (ref. 30),

is used to predict the boundary layer growth between regions of shock-wave boundary-layer interaction where either the analysis of Seebaugh, Paynter, and Childs (ref. 31) or Pinckney (ref. 32), is used. The Pinckney analysis is compatible with a possible separated region and was found to agree best with experiment where no bleed was present at the interaction. The Seebaugh, Paynter, Childs analysis considers three different bleed geometries: (1) porous, (2) flush slot, and (3) ram scoop. The model uses a control volume and solves for a boundary layer power profile consistent with the interaction pressure rise, the incoming momentum, and an assumption associated with the momentum removed with the bleed flow. Of the pressure and velocity terms for the momentum of the bleed flow entering the control volume, (1) the porous bleed case assumes both momentum terms add to the momentum of the remaining boundary layer flow exiting the control volume, (2) the flush slot case assumes the pressure term adds to the exiting boundary layer momentum and, (3) the ram scoop case assumes neither term adds to the boundary layer exit momentum. The experience at Lewis indicates that the third momentum assumption provides the best agreement with data for an oblique shock boundary layer interaction with porous bleed. A porous bleed stream tube model has been derived which is consistent with the later assumption. This approach avoids the necessity of assuming a "bleed efficiency" as proposed in reference 26.

The agreement of the analysis with measurements in an inlet employing isentropic and reflecting shock compression is shown in figure 9. Detailed surveys of the boundary layer were made at the five numbered locations and are the basis of the experimental values of displacement and momentum thicknesses and the incompressible shape factor and profile power. The method of Pinckney was used on the centerbody between 1 and 2 where no bleed was removed. The analysis of Seebaugh, Paynter, and Childs was used on the cowl and compared with cases where bleed was located upstream, across and downstream of the oblique shock reflections. In general, good agreement is demonstrated in five out of seven comparisons. At location 3, the displacement and momentum thicknesses are overpredicted, however, it is possible that the terminal shock could have affected the experimental values and it was not considered in the analysis. At location 5, good agreement is obtained between experiment and theory except for the case with bleed located upstream of the interaction, where the analysis predicted the bleed to be much more effective than shown by experiment. Bleed upstream of the interaction does not seem to be as effective as bleed located across or downstream of the interaction region where good agreement was obtained between experiment and analysis.

A comparison of predicted and measured profiles at the described stations is presented in figure 10. The trends discussed earlier are confirmed here. The lack of agreement at location 5 for upstream bleed is apparent. The agreement at location 5 for moderate and high bleed rates is also apparent when the bleed is located downstream of the shock reflection. Results for bleed located across the shock reflection region are similar to those for downstream bleed.

SUBSONIC DIFFUSER ANALYSIS

At the Lewis Research Center, a computer program has recently been acquired on contract to calculate the compressible viscous flow in an axisymmetric or two-dimensional subsonic diffuser. The program is an extension of the theory of ref. 33. Initial comparisons of the analysis with experimental inlet results as shown in figure 11, have provided confidence that the analysis is applicable to the diffuser of an axisymmetric inlet. This particular inlet was recently designed for use with a TF 30 engine at Mach 2.5. The main plot compares the experimental hub static pressure distribution (for the inlet with no vortex generator) with an inviscid calculation and results from the recently acquired viscous program. The good agreement is apparent, and demonstrates the necessity of having a good viscous analysis in order to obtain agreement with experimental pressure distributions. Also shown are two comparisons of total pressure profiles at the throat exit and the mid diffuser. Agreement is again good and separation in the actual inlet was accurately predicted by the computer program.

A small study was recently done utilizing this program to investigate the desirability of several different diffuser shapes. The axial pressure distribution for the three shapes studied is shown in the upper portion of figure 12. The boundary layer at the diffuser entrance is assumed in all cases to have a $1/7$ th power profile and the boundary layer displacement thickness for figure 12 provides a throat blockage of 1 percent. The three diffusers basically tradeoff high rates of compression at the upstream end of the diffuser where the velocities are high (which characterizes the "quadratic" diffuser) and resulting lower diffusion rates in the downstream region, with more uniform rates of diffusion throughout the diffuser length (constant $\frac{dm}{dx}$). The variation of skin friction coefficient on the hub is shown in the lower part of the figure. For the quadratic diffuser, the skin friction coefficient drops quickly within one throat height, but its rate

of decrease is reduced as the diffusion rate decreases and the program is able to complete the calculation while predicting very low skin friction coefficients over much of the diffuser length. For the constant dA/dx and dM/dx cases, much higher skin friction coefficients exist over most of the diffuser length, but at a distance from the throat of seven throat heights, the higher rates of diffusion separate the boundary layer and the calculation terminates. Therefore, for the healthy seventh power inlet profiles in the entering boundary layer, early high rates of diffusion appear to be beneficial. Figure 13 presents the effect of diffuser geometry in terms of more conventional diffuser parameter, the ratio of actual to ideal static pressure rise for the diffuser at the engine face. Diffusers of interest for supersonic inlets are only 10 to 20 throat heights long, but longer diffusers were studied to obtain solutions. The solid portion of the curves represent solutions completed to the compressor face and the dashed curves represent cases that were terminated due to flow separation. The three diffusers were studied with both 1 and 4 percent throat blockage. One percent blockage represents a rather heavily bled inlet while 4 percent blockage represents a rather low bleed condition. Only the quadratic diffuser with 1 percent blockage appears to be capable of operation without separation in the range of interest between 10 to 20 throat heights in length. Therefore, one desirable type of subsonic diffuser would be quadratic type with relative heavy bleed.

The advantages of such a diffuser are further demonstrated in figure 14 which presents the total pressure recovery of the diffuser (mass weighted) as a function of length. The recovery is either the value at the engine face for the unseparated cases (solid line) or the value at the point of incipient separation (dashed line). The quadratic diffuser again gives attached flow at shorter lengths for 1 percent blockage. Another interesting result is that at similar lengths, the constant dM/dx diffuser has considerably lower pressure recovery at the point of separation than the quadratic diffuser obtains at the compressor face. This is due to the lower average velocity and friction coefficient of the quadratic diffuser. However, this higher mass weighted total pressure recovery is probably not as surprising as the result that the higher rate of initial diffusion provides a higher static pressure rise and less tendency for boundary layer separation. This quadratic type of diffuser therefore appears to be quite interesting and potentially can provide an improvement in total pressure recovery. The results do indicate, however, that use of some boundary layer flow energizing device such as vortex generators will probably be required for diffusers of interesting length. Particularly when low inlet bleed rates are used.

CONCLUDING REMARKS

In evaluating the effect of inlet aerodynamic characteristics on supersonic cruise range, it becomes apparent that there is a broad range of potential inlet designs that are competitive. There are also other inlet characteristics such as angle of attack tolerance, airflow matching characteristics, weight, and complexity which will affect the inlet choice. Also, since the inlet study must involve consideration of airframe requirements as well as inlet characteristics, the resulting optimum inlet is not obvious. This conclusion is verified by observing the inlets chosen by the various airframe manufacturers for SST applications. Therefore the emphasis on inlet research should be to develop design methods for handling the viscous and inviscid flows in all the potential inlets of interest. This analysis effort must be accompanied by an experimental test program to provide verification of available analysis and guidance for future work.

Several examples of existing analytical computer programs for predicting inlet flows are available which can handle axisymmetric viscous flow in the supersonic and subsonic diffuser. While they represent a significant capability, they need to be extended. The transonic throat flow cannot be accurately calculated. Also, three-dimensional flow field calculations are needed for the combined viscous and inviscid flow fields in the supersonic and subsonic diffuser. With the development of these design tools, inlet angle of attack and the three-dimensional aspects of two-dimensional inlets could be accurately calculated. The resulting computing capability would provide the means to execute design studies which would provide the optimum inlet for a given set of design requirements.

REFERENCES

1. Calogeras, J. E., and Meleason, E. T., "Wind-Tunnel Investigation of Techniques for Reducing Cowl Drag of an Axisymmetric External-Compression Inlet at Mach 2.49," TM X-1516, 1968, NASA, Cleveland, Ohio.
2. Cubbison, R. W., Meleason, E. T., and Johnson, D. F., "Effect of Porous Bleed in a High-Performance Axisymmetric, Mixed-Compression Inlet at Mach 2.50," TM X-1692, NASA, Cleveland, Ohio.
3. Cubbison, R. W., Meleason, E. T., and Johnson, D. F., "Performance Characteristics from Mach 2.58 to 1.98 of an Axisymmetric Mixed-Compression Inlet System With 60-Percent Internal Contraction," TM X-1739, 1969, NASA, Cleveland, Ohio.
4. Wasserbauer, J. F., and Choby, D. A., "Mach 2.5 Performance of a Bicone Inlet With Internal Focused Compression and 40 Percent Internal Contraction," TM X-2294, 1971, NASA, Cleveland, Ohio.
5. Wasserbauer, J. F., and Choby, D. A., "Performance of a Bicone Inlet Designed for Mach 2.5 With Internal Distributed Compression and 40-Percent Internal Contraction," TM X-2416, 1972, NASA, Cleveland, Ohio.
6. Smeltzer, D. B., and Sorensen, N. E., "Tests of a Mixed Compression Axisymmetric Inlet With Large Transonic Mass Flow at Mach Numbers 0.6 to 2.65," TN D-6971, 1972, NASA, Moffett Field, Calif.
7. Koncsek, J. L., and Syberg, J., "Transonic and Supersonic Test of a Mach 2.65 Mixed-Compression Axisymmetric Intake," CR-1977, NASA, Washington, D.C.
8. Syberg, J., and Koncsek, J. L., "Transonic and Supersonic Test of the SST Prototype Air Intake," FAA-SS-72-50, 1972, FAA, Washington, D.C.
9. Anderson, W. E., and Wong, N. D., "Experimental Investigation of a Large-Scale, Two-Dimensional, Mixed-Compression Inlet System-Performance at Design Conditions, $M_\infty = 3.0$," TM X-2016, 1970, NASA, Moffett Field, Calif.
10. Smeltzer, D. B., and Sorensen, N. E., "Investigation of a Nearly Isentropic Mixed-Compression Axisymmetric Inlet System at Mach Numbers 0.6 to 3.2," TN D-4557, 1968, NASA, Moffett Field, Calif.
11. Sorensen, N. E., and Smeltzer, D. B., "Investigation of a Large-Scale Mixed-Compression Axisymmetric Inlet System Capable of High Performance at Mach Numbers 0.6 to 3.0," TM X-1507, 1968, NASA, Moffett Field, Calif.

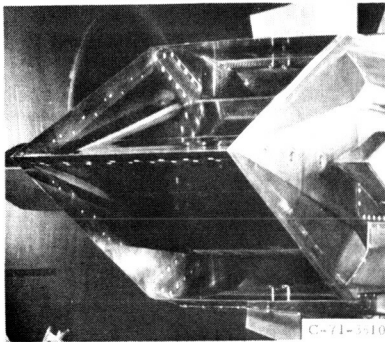
12. Bowditch, D. W., and Anderson, B. H., "Investigation of the Performance and Control of a Mach 3.0, Two-Dimensional, External-Internal-Compression Inlet," TM X-470, NASA, Cleveland, Ohio.
13. Smeltzer, D. B., and Sorensen, N. E., "Investigation of a Mixed-Compression Axisymmetric Inlet System at Mach Numbers 0.6 to 3.5," TN D-6078, 1970, NASA, Moffett Field, Calif.
14. Syberg, J., and Hickcox, T. E., "Design of a Bleed System for a Mach 3.5 Inlet," CR-2187, 1973, NASA, Washington, D.C.
15. Mitchell, G. A., and Cubbison, R. W., "An Experimental Investigation of the Restart Area Ratio of a Mach 3.0 Axisymmetric Mixed-Compression Inlet," TM X-1547, 1968, NASA, Cleveland, Ohio.
16. Anderson, B. H., "Characteristic Design Study of Mixed-Compression Two-Dimensional Inlets With Low-Angle Cowls for the Mach Number 2.70 to 1.80," TN D-5330, 1969, NASA, Cleveland, Ohio.
17. Anderson, B. H., "Characteristics Study of a Bicone Mixed-Compression Inlet for Mach 1.80 to 2.50," TN D-5084, 1969, NASA, Cleveland, Ohio.
18. Anderson, B. H., "Optimization of Supersonic Inlets Using the Method of Characteristics," "Analytical Methods in Aircraft Aerodynamics", SP-228, 1970, NASA, Washington, D.C., pp. 569-581.
19. Anderson, B. H., "Design of Supersonic Inlets by a Computer Program Incorporating the Method of Characteristics," TN D-4960, 1969, NASA, Cleveland, Ohio.
20. Sorensen, V. L., "Computer Program for Calculating Flow Fields in Supersonic Inlets," TN D-2897, 1965, NASA, Moffett Field, Calif.
21. Sorensen, N. E., Smeltzer, D. B., and Cubbison, R. W., "Study of a Family of Supersonic Inlet Systems, Journal of Aircraft, Vol. 6, No. 3, May-June, 1969, pp. 184-188.
22. Bowditch, D. N., Coltrin, R. E., Sanders, B. W., Sorensen, N. C., and Wasserbauer, J. F., Aircraft Propulsion, SP-259, 1971, NASA, Washington, D.C., pp. 283-312.
23. Sorensen, N. E., and Smeltzer, D. B., "Performance Estimates for a Supersonic Axisymmetric Inlet System," Journal of Aircraft, Vol. 9, No. 10, Oct. 1972, pp. 703-706.

24. Sanders, B. W., and Mitchell, G. A., "Increasing the Stable Operating Range of a Mach 2.5 Inlet," Paper 70-686, June 1970, AIAA, New York, N.Y.
25. Choby, D. A., "Tolerance of Mach 2.50 Axisymmetric Mixed-Compression Inlets to Upstream Flow Variations," TM X-2433, 1972, NASA, Cleveland, Ohio.
26. Reyhner, T. A., and Hickox, T. E., "Combined Viscous-Inviscid Analysis of Supersonic Inlet Flowfields," Journal of Aircraft, Vol. 9, No. 8, Aug. 1972, pp. 589-595.
27. Syberg, J., and Kancsek, S. L., "Bleed System Design Technology for Supersonic Inlets," Journal of Aircraft, Vol. 10, No. 7, July 1973, pp. 407-413.
28. Sorensen, N. E., Smeltzer, D. B., and Lathen, E. A., "Advanced Supersonic Inlet Technology," Journal of Aircraft, Vol. 10, No. 5, May 1973, pp. 278-282.
29. Hingst, W., and Towne, C., "Comparison of Theoretical and Experimental Boundary Layer Development in a Mach 2.5 Mixed-Compression Inlet," Proposed NASA Technical Memorandum.
30. McDonald, H., and Fish, R. W., "Practical Calculations of Transitional Boundary Layers," Boundary Layer Effects in Turbomachines, AGARDograph 164, 1972, pp. 29-54.
31. Seebaugh, W. R.; Payner, G. C.; Childs, M. E., "Calculation of Turbulent Boundary Layer Characteristics Across an Oblique Shock Reflection Including the Effects of Mass Bleed," Journal of Aircraft, Vol. 5, No. 5, Sept.-Oct. 1968, pp. 461-467.
32. Pinckney, S. Z., "Semiempirical Method for Prediction Effects of Incident-Reflecting Shocks on the Turbulent Boundary Layer," TN D-3029, 1965, NASA, Langley Station, Va.
33. Anderson, O. L., "A comparison of Theory and Experiment for Incompressible, Turbulent, Swirling Flows in Axisymmetric Ducts," Paper 72-43, Jan. 1972, New York, N.Y.

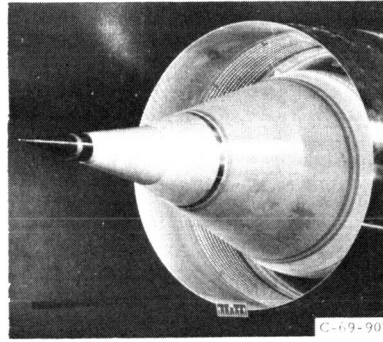
TABLE I.

Inlet	M_{DES}	$\frac{A_w(a)}{A_{th}}$	$\frac{A_w}{A_C}$	$\frac{P_{th}}{P_0}$	$\frac{\Delta A_{Si}}{\Delta A_S}$	$\frac{m_b}{m_0}$	$\frac{Opt}{P_2/P_0}$	α_{max}	$\frac{A_{th}}{A_C} \Bigg _{max}$	Type
TM X-1692	2.5	14.2	5.64	0.99	0.650	0.064	0.910	2.7	0.760	axisymmetric
TM X-2294	2.5	8.84	3.51	.98	.475	.050	.890	8.6	.755	axisymmetric
TM X-2416	2.5	12.19	4.84	.98	.475	.060	.925	3.6	.755	axisymmetric
NASA-Lewis	2.5	8.51	3.38	.98	.475	.025	.905	3.0	.755	axisymmetric
NASA-Lewis	2.5	7.84	3.11	.939	.0	-----	-----	---	.881	2D, AR = 0.81
TM X-1516	2.5	3.52	1.40	.99	.0	.056	.895	---	.430	axisymmetric
TN D-6971	2.65	19.11	6.59	.99	.795	.081	.944	1.9	.585	axisymmetric
CR-1977	2.65	18.82	6.49	.99	.778	.078	.936	2.0	.585	axisymmetric
FAA-SS-72-50	2.65	18.59	6.41	.99	.755	.066	.930	1.7	.635	axisymmetric
NASA-Lewis	2.7	17.94	5.90	.976	.350	.084	.900	2.4	.645	2D, AR = 1.565
NASA-Lewis	2.7	31.10	10.23	.973	.450	-----	-----	---	.620	2D, AR = 0.755
TM X-2016	3.0	39.44	9.75	.95	.610	.140	.895	1.0	.500	2D, AR = 1.0
TN D-4557	3.0	24.39	6.03	.99	.700	.095	.920	2.7	.390	axisymmetric
TM X-1507	3.0	23.54	5.82	.99	.625	.085	.894	3.0	.405	axisymmetric
TM X-470	3.0	28.19	6.97	.96	.406	.120	.890	2.0	.513	2D, AR = 0.775
TN D-6078	3.5	40.14	6.19	.99	.666	.138	.845	1.9	.335	axisymmetric
CR-2187	3.5	48.51	7.48	.99	.610	-----	-----	---	.435	axisymmetric

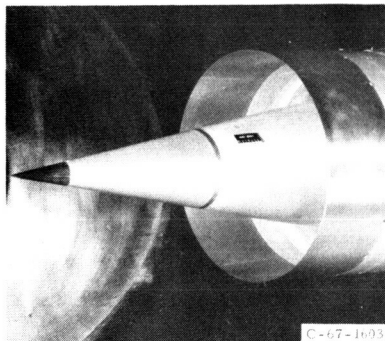
^a assumes $M_{th} = 1.25$



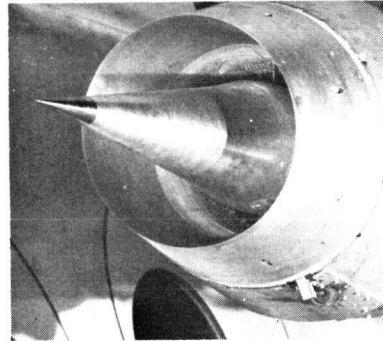
35 PERCENT INTERNAL COMPRESSION



48 PERCENT INTERNAL COMPRESSION



65 PERCENT INTERNAL COMPRESSION



80 PERCENT INTERNAL COMPRESSION

CS-68483

Figure 1. - Supersonic cruise inlets.

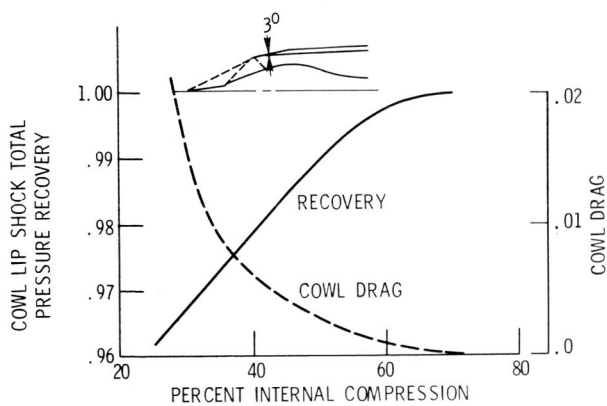


Figure 2. - Variation of total pressure recovery and cowl drag with internal compression. Optimized cowl lip angle. $M_0 = 2.5$.

CS-68486

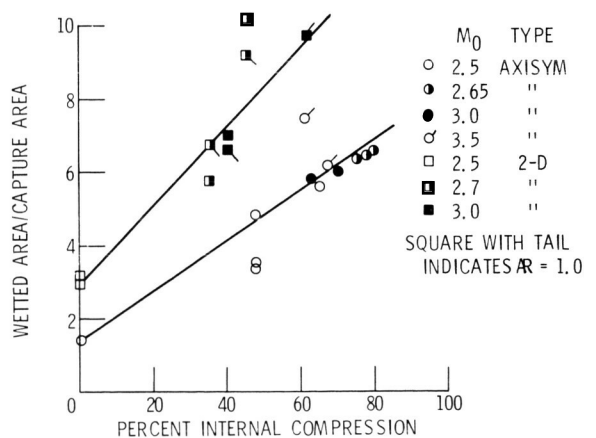


Figure 3. - Variation of wetted area with inlet internal compression.

CS-68489

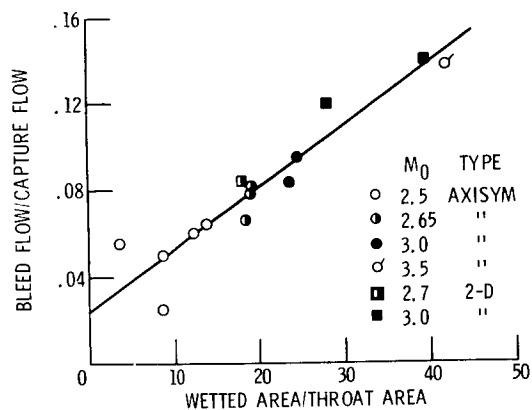


Figure 4. - Variation of bleed flow with wetted area at design Mach number.

CS-68487

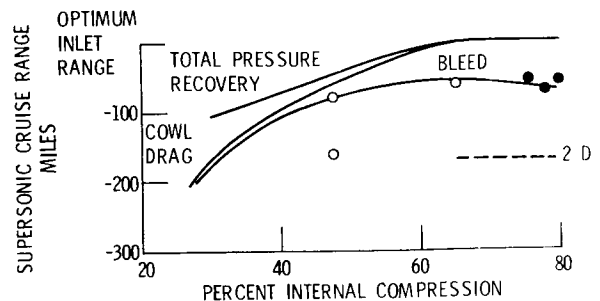


Figure 5. - Variation of supersonic cruise range with internal compression. $M_0 = 2.5$; $C_{D,MIN} = 0.0306$; $m_B/m_0 = 0.04$; $P_6/P_0 = 0.20$.

CS-68484

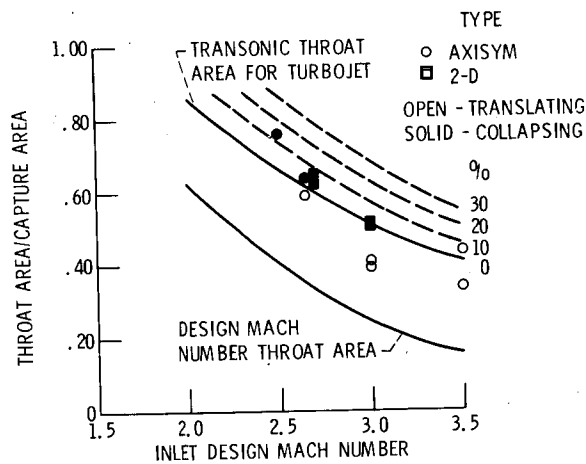


Figure 6. - Supersonic inlet matching capability.

CS-68490

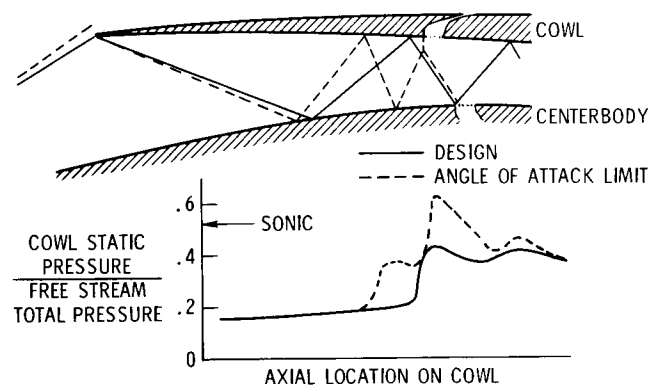


Figure 7. - Unstart limit for inlet angle of attack. Axisymmetric inlet.

CS-68492

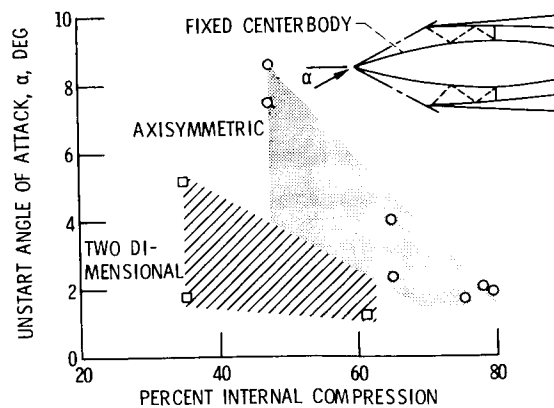
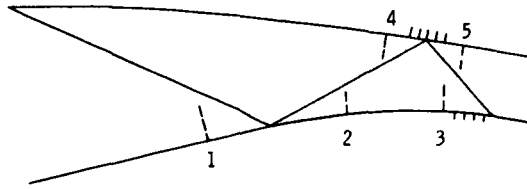


Figure 8. - Angle of attack limits for inlets. $M_0 = 2.5$ to 3.

CS-68488



PROBE	δ^* , CM		θ , CM		H_i		N_i	
	EXPER	THEORY	EXPER	THEORY	EXPER	THEORY	EXPER	THEORY
1	0.115	0.133	0.033	0.037	1.30	1.45	6.7	4.4
2	.134	.159	.049	.058	1.48	1.44	4.1	4.6
3	.117	.174	.048	.067	1.38	1.41	5.2	4.84
4	.078	.090	.029	.033	1.43	1.47	4.7	4.29
5 (UPSTREAM)	.080	.040	.040	.019	1.55	1.37	3.7	5.36
5 (ACROSS)	.053	.050	.026	.024	1.37	1.39	5.4	5.18
5 (DOWNSTREAM)	.075	.060	.036	.028	1.43	1.40	4.6	4.95

Figure 9. - Comparison of predicted and experimental inlet boundary layer.

CS-68496

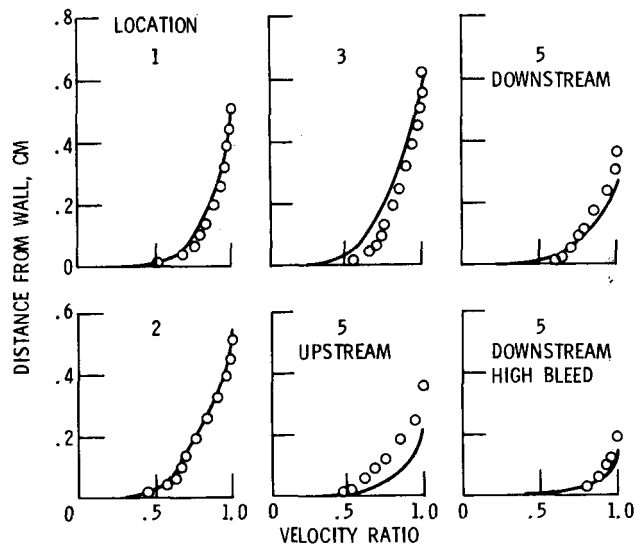


Figure 10. - Comparison of predicted and experimental boundary layer profiles.

CS-68493

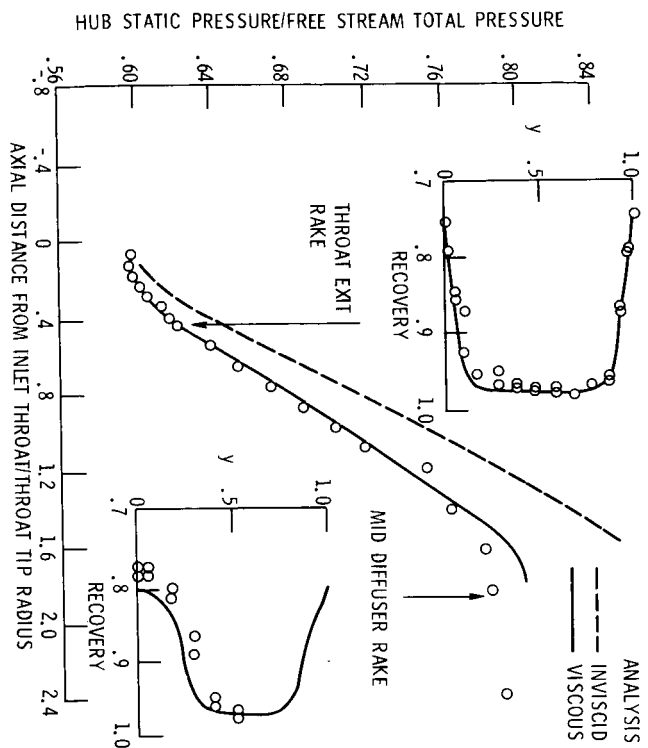


Figure 11. - Performance of subsonic diffuser for the TF30 inlet.

CS-68495

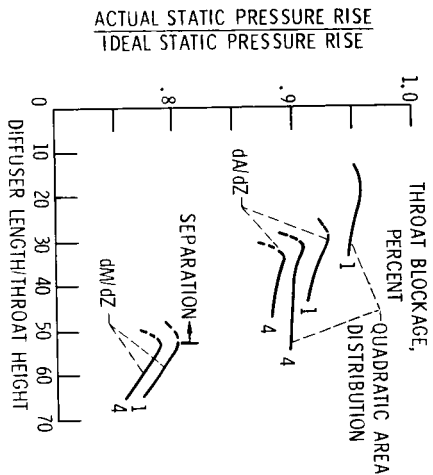


Figure 13. - Effect of annular diffuser geometry on effectiveness. Area ratio, 2.06.

CS-68495

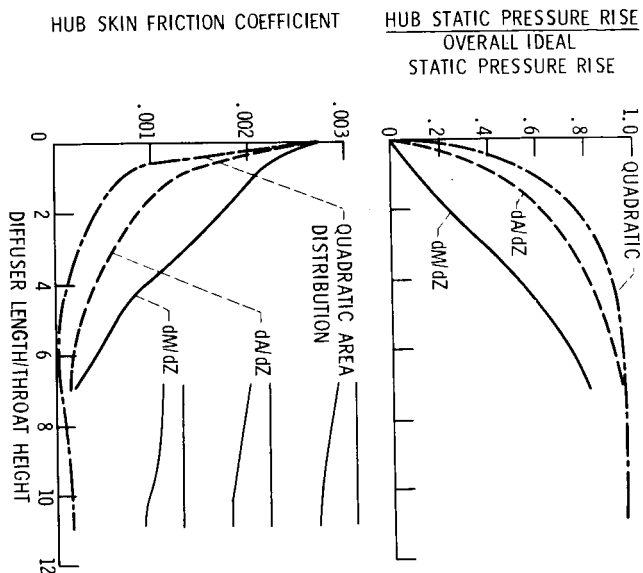


Figure 12. - Effect of annular diffuser geometry, 1 percent blockage. Area ratio, 2.06.

CS-68494

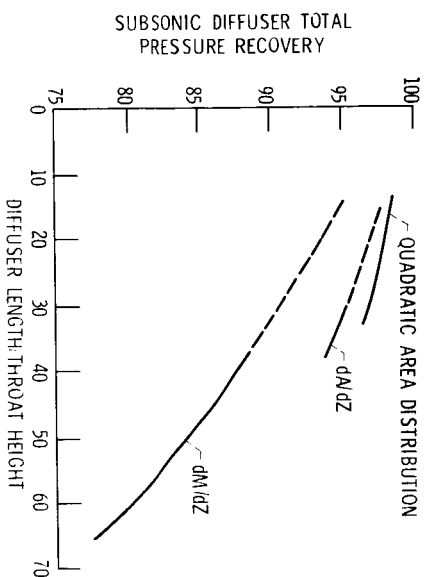


Figure 14. - Effect of annular diffuser geometry on total pressure recovery. Throat blockage, 1 percent; area ratio, 2.06.

CS-68494